Nuclear Instruments and Methods in Physics Research A 821 (2016) 136–141

Contents lists available at ScienceDirect

Nuclear Instruments and Methods in Physics Research A

journal homepage: www.elsevier.com/locate/nima

Excitation functions of the $^{nat}Cr(p,x)^{44}Ti$, $^{56}Fe(p,x)^{44}Ti$, $^{nat}Ni(p,x)^{44}Ti$ and $^{93}Nb(p,x)^{44}Ti$ reactions at energies up to 2.6 GeV

Yu. E. Titarenko [a,*], V.F. Batyaev [a], K.V. Pavlov [a], A. Yu. Titarenko [a], V.M. Zhivun [a,b], M.V. Chauzova [a], S.A. Balyuk [a], P.V. Bebenin [a], A.V. Ignatyuk [a,c], S.G. Mashnik [d], S. Leray [e], A. Boudard [e], J.C. David [e], D. Mancusi [e], J. Cugnon [f], Y. Yariv [g], K. Nishihara [h], N. Matsuda [h], H. Kumawat [i], A. Yu. Stankovskiy [j]

[a] National Research Center Kurchatov Institute, Institute for Theoretical and Experimental Physics, Moscow 117218, Russia
[b] National Research Nuclear University MEPhI (Moscow Engineering Physics Institute), Moscow 115409, Russia
[c] Institute of Physics and Power Engineering, Obninsk 249033, Russia
[d] Los Alamos National Laboratory, USA
[e] CEA/Saclay, Irfu/SPhN, 91191 Gif-sur-Yvette, Cedex, France
[f] University of Liege, Belgium
[g] SoreqNRC, Yavne, Israel
[h] JAEA, Tokai, Japan
[i] BARC, Mumbai, India
[j] SCK · CEN, Belgium

ARTICLE INFO

Article history:
Received 1 October 2015
Received in revised form
9 March 2016
Accepted 13 March 2016
Available online 16 March 2016

Keywords:
Cumulative yields
Proton beam
Excitation functions
Codes
Predictive power

ABSTRACT

The paper presents the measured cumulative yields of ^{44}Ti for ^{nat}Cr, ^{56}Fe, ^{nat}Ni and ^{93}Nb samples irradiated by protons at the energy range 0.04–2.6 GeV. The obtained excitation functions are compared with calculations of the well-known codes: ISABEL, Bertini, INCL4.2+ABLA, INCL4.5+ABLA07, PHITS, CASCADE07 and CEM03.02. The predictive power of these codes regarding the studied nuclides is analyzed.

1. Introduction

Accumulation of ^{44}Ti data in different materials can be interesting for various areas of science and technology. For example, the ^{44}Ti activity in meteorites is used effectively in astrophysics to study the century-scale variations of solar activity [1,2]. Natural titanium is also considered as the basic component of the developing low-activated V–Ti–Cr alloys of structural materials for advanced fusion reactors, which should work effectively in conditions of high neutron fluxes and high temperature regimes. ^{44}Ti will be important component of the long-lived residual radioactivity of such materials that will transform in the dominated one after about 3 years of a cooling-down time [3,4].

This paper presents the study of the cumulative production cross-sections of ^{44}Ti for ^{nat}Cr, ^{56}Fe, ^{nat}Ni and ^{93}Nb targets irradiated by protons at the energy range 0.04–2.6 GeV. Irradiations have been performed at the synchrophasotron of the Institute for Theoretical and Experimental Physics (ITEP) during the period from September 1, 2006 to August 31, 2009 within the framework of the International Science Technical Center Project #3266. Irradiation conditions and the measured independent and cumulative cross-sections of the reaction products are presented in Refs. [5–7]. On the whole 31 excitation functions for ^{nat}Cr, 39 excitation functions for ^{56}Fe, 47 excitation functions for ^{nat}Ni, and 109 excitation functions for ^{93}Nb have been determined. However, due to the high activity of the irradiated samples and the low energy gamma-lines from ^{44}Ti, the excitation function of this nuclide has not been determined in the previous measurements.

In order to obtain it, the measurements of gamma-spectra for the previously irradiated samples of ^{nat}Cr, ^{56}Fe, ^{nat}Ni and ^{93}Nb were continued in 2012–2015. The long cooling time provides a significant decrease in the radioactivity background due to the natural decay of the reaction products with short half-lives, and

* Corresponding author.

http://dx.doi.org/10.1016/j.nima.2016.03.046
0168-9002/

that allowed us to identify ^{44}Ti quite confidently by its distinctive gamma-lines.

2. Methodology

The gamma-ray spectra measurements of residual nuclei were performed by a spectrometer consisting of a low-energy Ge detector of the GUL0110 type with a resolution of 500 eV at the ^{57}Co gamma-line energy of 122 keV and the digital spectrum analyzer DSA1000. The absolute efficiency of the spectrometer was calibrated by means of the validated gamma-sources: ^{55}Fe, ^{241}Am, ^{133}Ba, ^{57}Co, ^{137}Cs, ^{44}Ti, which were certified by the Mendeleev Institute for Metrology (St. Petersburg, Russia). An example of such calibration is shown in Fig. 1. The background spectrum of the room in which the measurements were carried out is shown in Fig. 2.

The yield of ^{44}Ti ($T_{1/2}$=59.1y) was identified in accordance with the intensity of its attendant gamma-lines: 67.868 keV (93.0%) and 78.323 keV (96.4%) [8]. The third gamma-line satelliting the ^{44}Ti decay with energy 146.22 keV (0.092%) is not used because of its extremely low yield. The typical gamma-spectrum of ^{56}Fe sample irradiated by 0.4 GeV protons is shown in Fig. 3, which demonstrates a good separation of the dominant gamma-lines and a very low contribution of the third gamma-line. The gamma-spectra for the ^{nat}Cr, ^{56}Fe, ^{nat}Ni and ^{93}Nb samples measured at about 7 years after irradiation are very similar to the shown one and differ only by some changes of the dominant lines intensities.

The methodology for determining the cross-sections of radioactive reaction products by means of the gamma-ray spectrometry is described in details in Refs. [5–7]. Because ^{44}Ti has only short-lived precursors (see Fig. 4), the formula for the cumulative production rate for the i-th gamma-line (i=1, 2 for 67.868 and 78.323 keV lines, respectively) can be written as

$$R^i_{cum} = \frac{A_i}{N_{Tag}\cdot\eta_i\cdot\epsilon_i\cdot\lambda}\cdot\frac{1}{t_{irr}}, \quad (1)$$

where A_i is the count rate of the corresponding gamma-line reduced to the end of an exposure and adjusted to a self-absorption in the sample in accordance with the data of Ref. [9]; N_{Tag} is the number of nuclei in the sample, η_i is the absolute yield of the gamma-line per decay of ^{44}Ti; ε_i is the absolute efficiency of the spectrometer for the analyzed gamma-energy; λ is the decay constant of ^{44}Ti and t_{irr} is the irradiation time (since $t_{irr} << T^{44Ti}_{1/2}$, a correction for ^{44}Ti decay during irradiation can be ignored).

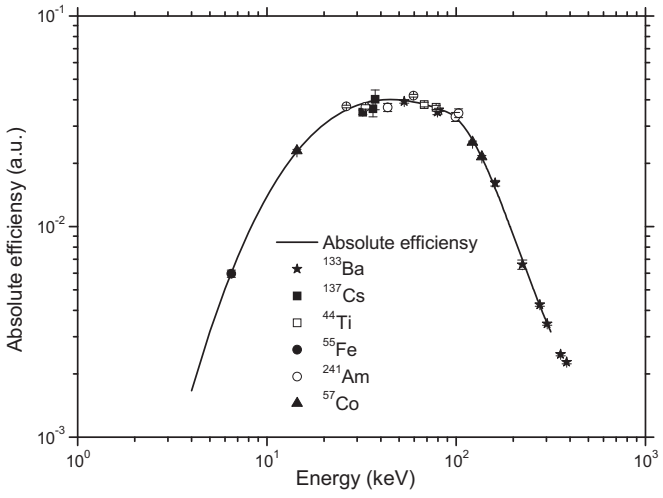

Fig. 1. Efficiency of the gamma-ray spectrometer with the Ge detector.

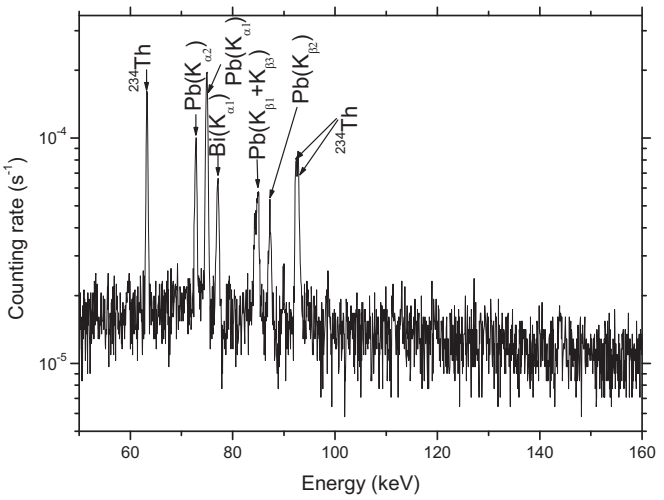

Fig. 2. The laboratory background spectrum. The measuring time was about 18 days.

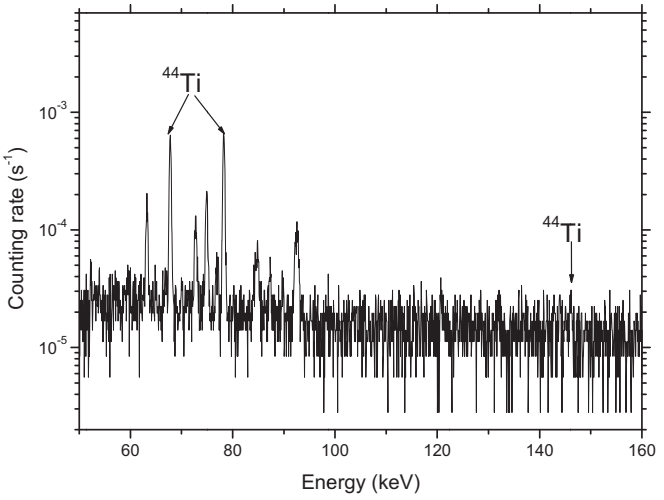

Fig. 3. The measured gamma-spectrum of the ^{56}Fe sample at about 7 years after irradiation by 0.4 GeV protons. The measuring time was about 99 h.

The reaction rate of the ^{44}Ti production was determined for each gamma-line, therefore to calculate the average value of the ^{44}Ti cumulative production rate the Eq. (2) has been applied while Eq. (3) has been used to calculate the corresponding production cross-sections:

$$\overline{R}^{44Ti}_{cum} = \frac{\sum_{i=1}^{2} R^i_{cum}\cdot W_i}{\sum_{i=1}^{2} W_i}., \text{ where } \quad W_i = \frac{1}{\left(\Delta R^i_{cum}\right)^2}\cdot \quad (2)$$

$$\sigma^{44Ti}_{cum} = \frac{\overline{R}^{44Ti}_{cum}}{\Phi_{st}} \quad (3)$$

here $\overline{R}^{44Ti}_{cum}$ is the averaged value of the cumulative production rate; ΔR^i_{cum} is the uncertainty of the gamma-line intensity estimation; σ^{44Ti}_{cum} denotes the ^{44}Ti production cross section and Φ_{st} is the proton flux presented in Tables 1–4 of Ref. [5].

Uncertainties of ΔR^i_{cum}, $\Delta\overline{R}^{44Ti}_{cum}$, $\Delta\sigma^{44Ti}_{cum}$ have been calculated in accordance with formulas given in Ref. [10].

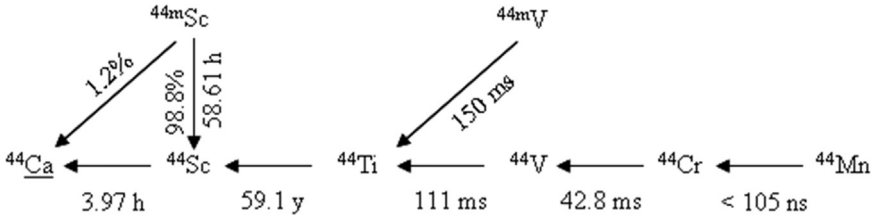

Fig. 4. The chain of the ^{44}Ti formation.

3. Experimental results

The obtained cross-sections for the ^{44}Ti production for all targets are summarized in Tables 1–4 together with their uncertainties.

4. Comparison with experimental results of other authors

The measured cumulative cross-sections for the ^{44}Ti production are shown in Figs. 5–8 together with the data compiled from Refs. [11–16].

The experimental database EXFOR [17] contains 5 entries [11–15] related to the ^{44}Ti production for the ^{nat}Fe target and 2 entries [11,12] for ^{nat}Ni. The ^{44}Ti production on ^{56}Fe is represented by only one experimental work [16] performed at GSI (Darmstadt) by means of the inverse kinematics (^{56}Fe→$^{1}_{1}$H). There are no EXFOR data on the ^{44}Ti production for the ^{nat}Cr and ^{93}Nb targets.

To compare the experimental data obtained by ITEP and other laboratories the mean-square deviation factor $\langle F\rangle$ has been considered, which closely corresponds to the widely-used statistical factors [18]:

$$\langle F\rangle = 10^{\left(\frac{1}{N}\sum_{i=1}^{N}\left[\log\left(\sigma_i^{exp}/\sigma_i^{ITEP}\right)\right]^2\right)^{1/2}} = 10^{\left(\left[\log\left(\overline{F}\right)\right]^2+\left[\log\left(\Delta\left(\overline{F}\right)\right)\right]^2\right)^{1/2}} \quad (4)$$

where σ_i^{exp} is the experimental data from [11–16]; σ_i^{ITEP} is the experimental results obtained by the ITEP group; N is the number of cross-sections used in a comparison. In the second form of Eq. (4) $\overline{F}$ is the averaged value of the lognormal distribution $\sigma_i^{exp}/\sigma_i^{ITEP}$ and $\Delta(\overline{F})$ is the dispersion of this distribution. Both of them are described by the following expressions:

$$\overline{F} = 10^{\frac{1}{N}\sum_{i=1}^{N}\left[\log\left(\sigma_i^{exp}/\sigma_i^{ITEP}\right)\right]} \quad (5)$$

$$\Delta(\overline{F}) = 10^{\left(\frac{1}{N}\sum_{i=1}^{N}\left[\log\left(\sigma_i^{exp}/\sigma_i^{ITEP}\right)-\log(\overline{F})\right]^2\right)^{1/2}} \quad (6)$$

The factors $\overline{F}$ and $\Delta(\overline{F})$ are widely used under the classical statistical analysis of data. They characterize the systematic shift between two sets of data and the common spread of data, respectively. On the other hand, the formula (4) reduces a two-parameter consideration to a one-parameter description, which could be more convenient for a simplified comparison of data and a graphical representation of data discrepancies.

Since the proton energies of the experimental data obtained by ITEP and Refs. [11–16] are not always coincided the ITEP data have been interpolated to the energies corresponding to [11–16]. The values of $\langle F\rangle$, $\overline{F}$ and $\Delta(\overline{F})$ calculated according to (Eqs. (4)–6) are shown in Table 5.

Small deviations of the statistical factors from a unit show a good agreement ($\lesssim$30%) between the ITEP results and the data of Refs. [11,12,15,16] for iron and Ref. [12] for nickel.

Table 1
Measured cross-sections for the reaction ^{nat}Cr(p,x)^{44}Ti.

Target	E_p, GeV	$\overline{R}^{44Ti}_{cum} \pm \Delta\overline{R}^{44Ti}_{cum}$, (1/s) × 10^{-17}	$\hat{\Phi}_{st} \pm \Delta\hat{\Phi}_{st}$, (p/(cm^2 s)) × 10^{10}	$\sigma^{44Ti}_{cum} \pm \Delta\sigma^{44Ti}_{cum}\sigma$, mb
Cr	0.07	2.20 ± 0.11	5.42 ± 0.43	0.405 ± 0.038
	0.1	5.21 ± 0.24	3.73 ± 0.28	1.40 ± 0.12
	0.15	5.11 ± 0.19	3.14 ± 0.27	1.63 ± 0.15
	0.25	11.57 ± 0.42	7.27 ± 0.64	1.59 ± 0.15
	0.4	9.93 ± 0.55	5.70 ± 0.47	1.74 ± 0.17
	0.6	12.94 ± 0.39	6.78 ± 0.52	1.91 ± 0.16
	0.8	10.67 ± 0.46	6.88 ± 0.64	1.55 ± 0.16
	1.2	9.32 ± 0.25	6.70 ± 0.54	1.39 ± 0.12
	1.6	7.42 ± 0.21	5.98 ± 0.50	1.24 ± 0.11
	2.6	3.96 ± 0.15	5.26 ± 0.46	0.753 ± 0.072

Table 2
Measured cross-sections for the reaction ^{56}Fe(p,x)^{44}Ti.

Target	E_p, GeV	$\overline{R}^{44Ti}_{cum} \pm \Delta\overline{R}^{44Ti}_{cum}$, (1/s) × 10^{-17}	$\hat{\Phi}_{st} \pm \Delta\hat{\Phi}_{st}$, (p/(cm^2 s)) × 10^{10}	$\sigma^{44Ti}_{cum} \pm \Delta\sigma^{44Ti}_{cum}\sigma$, m barn
Fe	0.1	0.30 ± 0.12	4.07 ± 0.31	0.073 ± 0.031
	0.15	0.98 ± 0.14	3.44 ± 0.30	0.284 ± 0.047
	0.25	4.63 ± 0.32	7.22 ± 0.51	0.641 ± 0.064
	0.3	5.20 ± 0.16	5.23 ± 0.38	0.994 ± 0.079
	0.4	7.13 ± 0.23	6.35 ± 0.57	1.12 ± 0.11
	0.6	11.00 ± 0.48	7.99 ± 0.64	1.38 ± 0.13
	0.75	11.88 ± 0.35	7.45 ± 0.64	1.59 ± 0.14
	0.8	9.22 ± 0.28	6.97 ± 0.59	1.32 ± 0.12
	1.2	9.03 ± 0.44	6.62 ± 0.53	1.36 ± 0.13
	1.6	7.80 ± 0.35	5.56 ± 0.47	1.40 ± 0.13
	2.6	4.51 ± 0.27	4.75 ± 0.41	0.95 ± 0.10

Table 3
Measured cross-sections for the reaction ^{nat}Ni(p,x)^{44}Ti.

Target	E_p, GeV	$\overline{R}^{44Ti}_{cum} \pm \Delta\overline{R}^{44Ti}_{cum}$, (1/s) × 10^{-17}	$\hat{\Phi}_{st} \pm \Delta\hat{\Phi}_{st}$, (p/(cm^2 s)) × 10^{10}	$\sigma^{44Ti}_{cum} \pm \Delta\sigma^{44Ti}_{cum}\sigma$, m barn
Ni	0.1	0.390 ± 0.084	4.36 ± 0.32	0.089 ± 0.020
	0.15	1.32 ± 0.20	5.31 ± 0.45	0.248 ± 0.044
	0.25	4.57 ± 0.39	7.10 ± 0.55	0.643 ± 0.074
	0.4	5.50 ± 0.41	4.01 ± 0.38	1.37 ± 0.17
	0.6	17.25 ± 0.73	7.19 ± 0.68	2.40 ± 0.25
	0.8	7.32 ± 0.40	3.06 ± 0.26	2.39 ± 0.24
	1.2	8.77 ± 0.44	3.39 ± 0.27	2.59 ± 0.24
	1.6	11.57 ± 0.54	5.30 ± 0.44	2.18 ± 0.21
	2.6	10.82 ± 0.54	6.45 ± 0.56	1.68 ± 0.17

Table 4
Measured cross-sections for the reaction ^{93}Nb(p,x) ^{44}Ti.

Target	E_p, GeV	$\overline{R}^{44Ti}_{cum} \pm \Delta\overline{R}^{44Ti}_{cum}$, (1/s) × 10^{-17}	$\hat{\Phi}_{st} \pm \Delta\hat{\Phi}_{st}$, (p/(cm^2 s)) × 10^{10}	$\sigma^{44Ti}_{cum} \pm \Delta\sigma^{44Ti}_{cum}\sigma$, m barn
Nb	1.2	0.054 ± 0.053	3.66 ± 0.29	0.015 ± 0.015
	1.6	0.50 ± 0.23	6.00 ± 0.50	0.084 ± 0.039
	2.6	0.76 ± 0.25	6.96 ± 0.61	0.109 ± 0.037

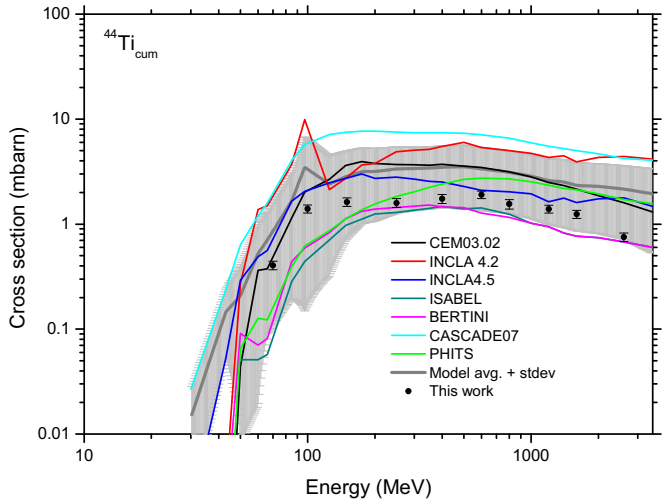

Fig. 5. Calculated cross-sections and experimental data for the reaction $^{nat}Cr(p,x)^{44}Ti_{cum}$.

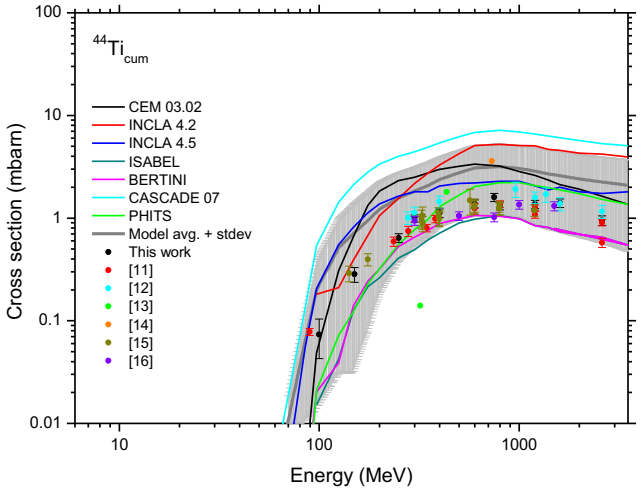

Fig. 6. Calculated cross-sections and experimental data for the reaction $^{56}Fe(p,x)^{44}Ti_{cum}$.

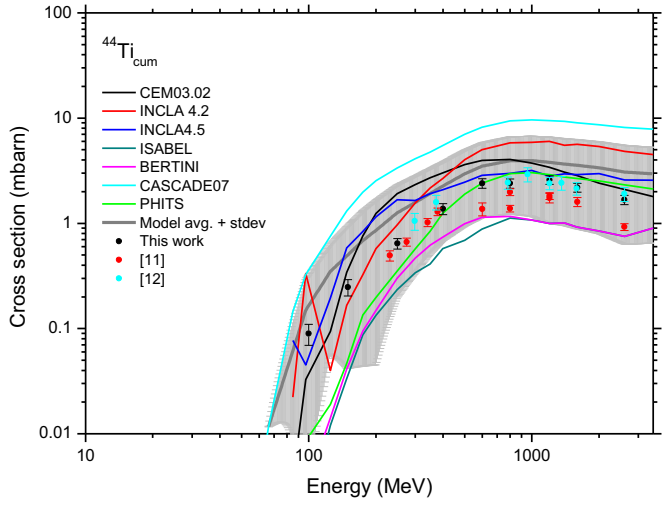

Fig. 7. Calculated cross-sections and experimental data for the reaction $^{nat}Ni(p,x)^{44}Ti_{cum}$.

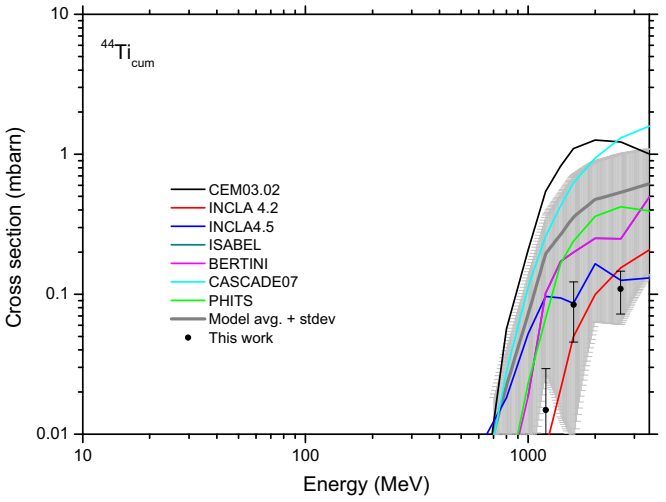

Fig. 8. Calculated cross-sections and experimental data for the reaction $^{93}Nb(p,x)^{44}Ti_{cum}$.

5. Comparison with model calculations

The production cross-sections of ^{44}Ti have been calculated using different versions of the intranuclear cascade model realized in the well-known codes: ISABEL, Bertini, INCL4.2+ABLA, INCL4.5+ABLA07, PHITS, CASCADE07, and CEM03.02. A brief overview of these codes is given in Refs. [18,19], and a detailed consideration of their main components can be found in the references collected in [5]. All these codes calculate the independent cross-sections of the residual nuclei while their cumulative production cross-sections must be calculated in accordance with the formulas presented in [5]. The calculated cumulative cross-sections for the ^{44}Ti production are presented in Figs. 5–8 together with the corresponding experimental data.

In addition to the calculated cross-sections, the averaged standard deviations of model results are shown as a grey background in Figs. 5–8. This allows to infer visually the quality of reproducing experimental data in the model calculations. For quantitative determination of predictive power of models for the ^{44}Ti cumulative cross-sections,-the statistical factors were calculated in accordance with (Eqs. (4)–6) with the replacement of σ_i^{exp} by the calculated values σ_i^{calc} obtained with the model codes. The calculated factors are presented in Table 6

The above statistical factors demonstrate that the discrepancy between the experimental results obtained in different laboratories is much lower than the discrepancy between model calculations and experimental data. The results of the INCL4.5+ABLA07 code look preferable over others and the CEM03.02 results show a similar quality for light targets but not for ^{93}Nb. This conclusion about the model codes correlated strongly with the general resume made before for a large amount of the high-energy excitation functions of the proton induced reactions [18].

6. Conclusion

New experimental data on the production cross-sections of the long-lived radionuclide ^{44}Ti for main components of the structural materials can be especially interesting for the analysis of the residual activity of the accelerator-driven system equipment that will work in conditions of high protons and neutron fluxes. On the other side, these data can be also useful for the ongoing

Table 5
Values of statistical factors for the data obtained in Refs. [11–16] and ITEP.

Target	Reaction product	Factors	Compared for Fe					
			[11], (N=11)	[12], (N=8)	[13], (N=2)	[14], (N=1)	[15], (N=17)	[16], (N=5)
^{56}Fe	^{44}Ti$_{cum}$	$\langle F\rangle$	1.27	1.23	4.21	2.69	1.11	1.18
		$\overline{F}$	0.91	1.20	0.46	2.69	0.96	0.87
		$\Delta(\overline{F})$	1.24	1.10	3.35	–	1.10	1.10
Target	Reaction product	Factors	Compared for Ni					
			[11], (N=10)	[12], (N=8)	–	–	–	–
^{nat}Ni	^{44}Ti$_{cum}$	$\langle F\rangle$	1.40	1.15				
		$\overline{F}$	0.77	1.09				
		$\Delta(\overline{F})$	1.22	1.12				

Table 6
Statistical factors of the model simulating the ^{44}Ti$_{cum}$ cumulative production cross-sections for ^{nat}Cr, ^{56}Fe, ^{nat}N, and ^{93}Nb samples irradiated by protons at the energy range 0.04–2.6 GeV.

Target	Reaction product	Factors	Code						
			CEM03.02	INCL4.2+ABLA	INCL4.5+ABLA07	ISABEL	BERTI-NI	CASCA-DE07	PHITS
^{nat}Cr	^{44}Ti$_{cum}$	$\langle F\rangle$	1.90	3.62	1.54	2.27	1.90	4.31	1.88
		$\overline{F}$	1.80	3.42	1.46	0.55	0.62	4.29	1.09
		$\Delta(\overline{F})$	1.30	1.46	1.23	1.75	1.54	1.12	1.87
^{56}Fe	^{44}Ti$_{cum}$	$\langle F\rangle$	2.25	2.93	1.98	2.08	1.84	5.34	1.74
		$\overline{F}$	1.95	2.80	1.87	0.53	0.60	5.27	0.94
		$\Delta(\overline{F})$	1.59	1.36	1.31	1.43	1.38	1.23	1.74
^{nat}Ni	^{44}Ti$_{cum}$	$\langle F\rangle$	1.89	2.35	1.72	5.53	4.28	4.23	2.71
		$\overline{F}$	1.39	2.05	1.36	0.25	0.31	4.19	0.65
		$\Delta(\overline{F})$	1.72	1.59	1.57	2.78	2.33	1.16	2.45
^{93}Nb	^{44}Ti$_{cum}$	$\langle F\rangle$	18.3	1.68	2.95	3.69	3.69	11.9	3.72
		$\overline{F}$	17.5	0.76	1.97	3.33	3.33	11.6	3.67
		$\Delta(\overline{F})$	1.69	1.55	2.33	1.66	1.66	1.42	1.21

development of the transport codes widely used for many applications. The predictive accuracy of some code versions certainly needs essential improvements.

Acknowledgments

The authors would like to thank the ITEP accelerator team for the long-time participation in irradiation of various samples as well as Prof. S. V. Rogozhkin, Prof. S. V. Stepanov and Prof. V.P. Kolotov for the fruitful discussion and valuable comments. The authors also appreciate the supports received from the International Science Technical Center (3266) (Moscow) and International Atomic Energy Agency (13397/R0 (Research Contract between the IAEA and ITEP)) (Vienna), as well as from the current pilot project of the National Research Center "Kurchatov Institute". Part of the work performed at Los Alamos National Laboratory was carried out under the auspices of the National Nuclear Security Administration of the U.S. Department of Energy (DE-AC52-06NA25396).

References

[1] C. Taricco, N. Bhandari, D. Cane, P. Colombetti, N. Verma, J. Geophys. Res. 111 (2006) A08102.
[2] G. Bonino, Nuovo Cimento C 16 (1993) 29.
[3] W.R. Johnson, J.P. Smith, J. Nucl. Mater. 258–263 (1998) 1425.
[4] A.K. Shikov, V.A. Beliakov, J. Nucl. Mater. 367–370 (2007) 1298.
[5] Yu. E. Titarenko, V.F. Batyaev, A.A. Belonozhenko, S.P. Borovlev, M.A. Butko, S.N. Florya, K.V. Pavlov, V.I. Rogov, R.S. Tikhonov, A. Yu. Titarenko, V.M. Zhivun, Experimental and Theoretical Study of the Residual Nuclide Production in 40 – 2600 MeV Proton-irradiated Thin Targets of ADS Structure Materials, IAEA, IAEA Nuclear Data Section, Vienna International Centre, A-1400 Vienna, Austria, INDC(CCP)-0453, October 2011.
[6] Yu. E. Titarenko, V.F. Batyaev, A. Yu Titarenko, M.A. Butko, K.V. Pavlov, S. N. Florya, R.S. Tikhonov, V.M. Zhivun, A.V. Ignatyuk, S.G. Mashnik, S. Leray, A. Boudard, J. Cugnon, D. Mancusi, Y. Yariv, K. Nishihara, N. Matsuda, H. Kumawat, G. Mank, W. Gudowski, Phys. Atom. Nucl. – Engl. Tr. 74 (2011) 523.
[7] E. Yu., V.F. Titarenko, A. Batyaev, Yu Titarenko, M.A. Butko, K.V. Pavlov, S. N. Florya, R.S. Tikhonov, V.M. Zhivun, A.V. Ignatyuk, S.G. Mashnik, S. Leray, A. Boudard, J. Cugnon, D. Mancusi, Y. Yariv, K. Nishihara, N. Matsuda, H. Kumawat, G. Mank, W. Gudowski, Phys. Atom. Nucl – Engl. Tr. 74 (2011) 537.
[8] Jun Chen, Balraj Singh, John A. Cameron, Nucl. Data Sheets 112 (9) (2011) 2357 ⟨http://www.nndc.bnl.gov/nudat2/indx_dec.jsp⟩.
[9] E. Storm, H.I. Israel, Nucl. Data Tables A7 (1970) 681.
[10] JCGM 100:2008, GUM 1995 with minor corrections, GUM Evaluation of measurement data — Guide to the expression of uncertainty in measurement, first ed., September 2008.
[11] R. Michel, R. Bodemann, H. Busemann, R. Daunke, M. Gloris, H.-J. Lange, B. Klug, A. Krins, I. Leya, M. Luepke, S. Neumann, H. Reinhardt, M. Schnatz-Buettgen, U. Herpers, Th Schiekel, F. Sudbrock, B. Holmqvist, H. Conde, P. Malmborg, M. Suter, B. Dittrich-Hannen, P.-W. Kubik, H.-A. Sinal, D. Filges, Nucl. Instrum. Methods B129 (1997) 153.
[12] S. Neumann, Activation Experiments with Medium-energy Neutrons and the Production of Cosmogenic Nuclides in Extraterrestrial Matter (Thesis or dissertation), 1999.
[13] R.L. Brodzinski, L.A. Rancitelli, J.A. Cooper, N.A. Wogman, Phys. Rev. C 4 (1971) 1257.
[14] M. Honda, D. Lal, Nucl. Phys. 51 (1964) 363.
[15] M. Gloris, Proton-induced production of residual nuclei in heavy elements at medium energies (Thesis or dissertation), 1998.
[16] C. Villagrasa-Canton, A. Boudard, J.-E. Ducret, B. Fernandez, S. Leray, C. Volant, P. Armbruster, T. Enqvist, F. Hammache, K. Helariutta, B. Jurado, M.-V. Ricciardi, K.-H. Schmidt, K. Summerer, F. Vives, O. Yordanov, L. Audouin, C.-O. Bacri, L. Ferrant, P. Napolitani, F. Rejmund, C. Stephan, L. Tassan-Got, J. Benlliure, E. Casarejos, M. Fernandez-Ordonez, J. Pereira, S. Czajkowski,

D. Karamanis, M. Pravikoff, J.S. George, R.A. Mewaldt, N. Yanasak, M. Wiedenbeck, J.J. Connell, T. Faestermann, A. Heinz, A. Junghans, Phys. Rev. C, 75, (2007) 044603.

[17] EXFOR: Experimental nuclear reaction data database, version of November 23, 2015, ⟨https://www-nds.iaea.org/exfor/exfor.htm⟩.

[18] Yu. E. Titarenko, V.F. Batyaev, M.A. Butko, D.V. Dikarev, S.N. Florya, K.V. Pavlov, A. Yu Titarenko, R.S. Tikhonov, V.M. Zhivun, A.V. Ignatyuk, S.G. Mashnik, A. Boudard, S. Leray, J.-C. David, J. Cugnon, D. Mancusi, Y. Yariv, H. Kumawat, K. Nishihara, N. Matsuda, G. Mank, W. Gudowski, Phys. Rev. C 84 (2011) 064612.

[19] D. Filges, S. Leray, Y. Yariv, A. Mengoni, A. Staculescu, G. Mank, Joint ICTP-IAEA Advanced Workshop on Model Codes for Spallation Reactions, IAEA, IAEA Nuclear Data Section, Vienna International Centre, A-1400 Vienna, Austria, INDC(NDS)-0530, August 2008.